PAPER

NJC
www.rsc.org/njc

Studies of Langmuir and Langmuir–Blodgett films of NLO-active amphiphilic 1,3-indanedione derivatives†

Somobrata Acharya,[ae] Pnina Krief,[a] Vladimir Khodorkovsky,*[ab] Zvi Kotler,[c] Gerry Berkovic,[c] Jacob T. Klug[d] and (the late) Shlomo Efrima[ae]

[a] *Department of Chemistry, Ben-Gurion University, Beer-Sheva, 84105, Israel. E-mail: hodor@bgu.ac.il; Fax: +972-8-6472943; Tel: +972-8-6472188*
[b] *Groupe de chimie organique et matériaux moléculaires (CNRS UMR 6114) Université de la Méditerranée, 13288 Marseille Cedex 9, France. E-mail: khodor@luminy.univ-mrs.fr; Fax: +33-4-91829301; Tel: +33-4-91829322*
[c] *Electro-Optics Div., Soreq Nuclear Research Center (NRC), Yavne, 81800 Israel. E-mail: zvi@soreq.gov.il; Tel: +972-8-9434104*
[d] *The Institutes for Applied Research, Ben-Gurion University, Beer-Sheva, 84105 Israel. E-mail: jklug@bgu.ac.il; Tel: +972-8-6461975*
[e] *The Ilse Katz Center for Meso and Nanoscale Science and Technology, Ben-Gurion University, Beer-Sheva, 84105, Israel. E-mail: acharya@bgu.ac.il; Tel: +972-8-6472173*

Received (in Montpellier, France) 30th March 2005, Accepted 10th June 2005
First published as an Advance Article on the web 7th July 2005

We studied Langmuir and Langmuir–Blodgett (LB) films of several strong nonlinear optical (NLO) active amphiphilic derivatives of 1,3-indanedione-5,6-dicarboxylic acid. The surface pressure–area (π–A) isotherms at the air–water interface were investigated at different temperatures and pH values. Non-centrosymmetric Z-type LB films were deposited. UV–visible spectra indicated a uniform film transfer. The orientation of the molecular transition moments was calculated from the polarized UV–visible spectra. Packing within the LB films was observed by UV–visible absorption and fluorescence spectroscopy. The morphology of the LB films was examined by AFM and compared to ellipsometric measurements, and the nature of the films was studied by contact angle measurements. Significant second harmonic generation (SHG) by the LB films was observed. Alternate layer Y-type LB films of two different dyes were fabricated to achieve enhanced stability and SHG.

Introduction

Fabrication of novel supramolecular structures with the ultimate goal of achieving molecular control of structure and function at the nano scale is at the core of nanoscience and nanotechnology and has prompted an increasing demand for the development of methods to assemble and characterize such structures.[1] Ultrathin films obtained by means of the Langmuir–Blodgett (LB) or self-assembly (SA) techniques have many potential applications, *e.g.*, in molecular photoelectronics, NEMs (nano electromechanical) devices, and miniaturized optics and biosensors.[2] The molecular architecture of these films affects their properties, which can be different from those manifested by the same materials in bulk. In fact, the properties of these films depend on both the characteristics of the molecules themselves, as well as on the manner of their association in the film. Hence there is a fundamental interest in assembling, controlling and understanding the molecular structure and organization in these films.

Molecules consisting of a donor (D) moiety linked by a conjugated bridge (π) to an acceptor (A) moiety have become the subject of intense interest due to their potential in nonlinear optical (NLO) applications.[3] The development of advanced materials for photonic applications based on second harmonic generation (SHG) requires addressing several major problems. The first is the design of the D–π–A chromophores with maximized hyperpolarizabilities. Such D–π–A materials can be optimized by varying the donor and acceptor groups, their relative position, and orientation in the molecule, as well as the length of the π-electron bridge.[4] In the previous work we studied Langmuir and LB films of several 1,3-indanedione derivatives, in particular, derivative **1** (Fig. 1),[5,6] as a prototype for potentially strong NLO chromophores. The second important issue when developing SHG systems is the assembly of these chromophores in a non-centrosymmetric arrangement in miniature nanoscale systems. This can be accomplished by fabrication of LB or SA films of the NLO-active chromophores, where the alignment and orientation of the chromophores might be controlled. LB films allow convenient assembly of multilayers, but these films might be relatively unstable, as is usual when van der Waals forces are involved.

SA films, on the other hand, are usually more stable, but the assembly of multilayers is more difficult requiring specific chemical reactions (and often chemical protection stages of some of the groups to prohibit reactions in solution).

Recently, we developed a synthetic procedure for the synthesis of previously unknown 1,3-indanedione-5,6-dicarboxylic acid, as a precursor for a variety of water soluble 1,3-indanedione derivatives.[7] In the present work we studied Langmuir and LB films of long chain substituted derivatives of 1,3-indanedione-5,6-dicarboxylic acid **2a–2d** (Fig. 2). These compounds are newly developed materials with high NLO activity

† Electronic supplementary information (ESI) available: Derivation of dichroic analysis of polarized UV–visible absorption spectrum. See http://dx.doi.org/10.1039/b504445f

DOI: 10.1039/b504445f

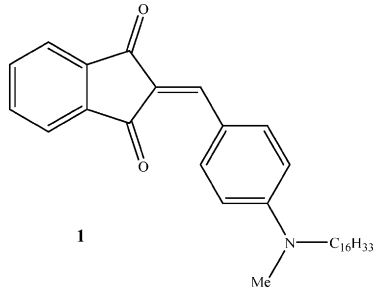

Fig. 1 Molecular structure of 2-{4-[hexadecyl(methyl)amino]benzylidene}-1*H*-indene-1,3(2*H*)-dione (**1**), a prototype NLO-active chromophore.

involving the 1,3-indanedione 2-ylidene moiety bearing two extra electron accepting substituents as an acceptor (A) and the *p*-dialkylaminophenyl moiety as a donor. Increase in the electron accepting properties of the 1,3-indanedione moiety is evidenced, in particular, by the pronounced red shift of the charge transfer absorption bands of the corresponding D–A derivatives compared to the unsubstituted analogs.[7] The two carboxylic groups on the 1,3-indanedione moiety not only enhance the NLO activity, but also the hydrophilic nature of the head-group, compared to the prototype molecule **1**.[5,8] Attaching a long-chain alkyl group as the hydrophobic tail on the electron donating moiety (**2a** and **2b**) or on the electron accepting moiety (**2c** and **2d**) imparts an amphiphilic character

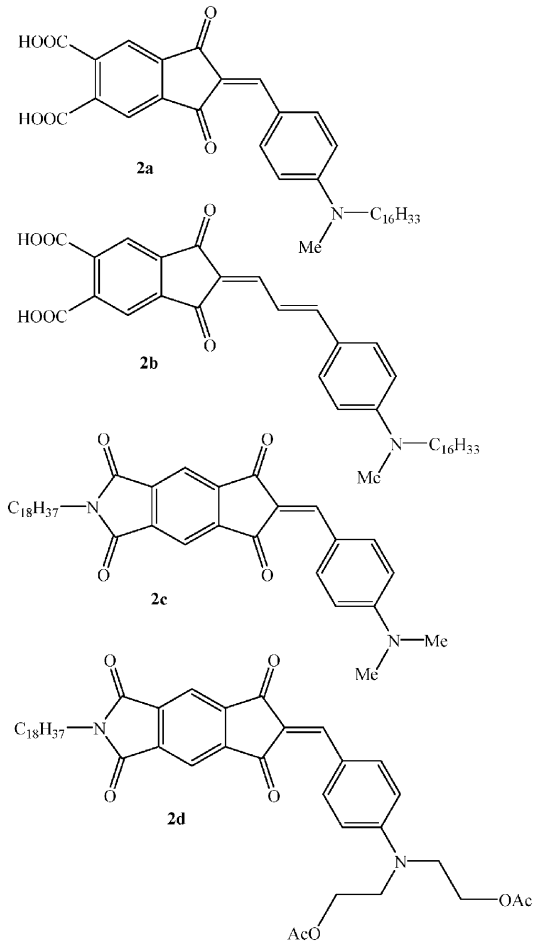

Fig. 2 Molecular structure of 2-(4-[hexadecyl(methyl)amino]phenylmethylene)-1,3-dioxo-5,6-indanedicarboxylic acid (**2a**), 2-((*E*)-3-{4-[hexadecyl(methyl)amino]phenyl}-2-propenylidene)-1,3-dioxo-5,6-indanedicarboxylic acid (**2b**), 6-[4-(dimethylamino)benzylidene]-2-octadecylcyclopenta[*f*]isoindole-1,3,5,7(2*H*,6*H*)-tetrone (**2c**), ({4-[(2-octadecyl-1,3,5,7-tetraoxo-2,3,5,7-tetrahydrocyclopenta[*f*]isoindol-6(1*H*)-ylidene)methyl]phenyl}imino)bis(ethane-2,1-diyl) diacetate (**2d**).

to the molecule incorporating the NLO chromophore. These amphiphiles should form stable Langmuir films and subsequently LB films.

We first studied the isotherms of the Langmuir monolayers of these molecules. On the basis of this study, optimal conditions for deposition of the LB films were identified and the LB films were prepared. Characterization of the LB films was carried out using UV–visible absorption, polarized absorption, ellipsometry, fluorescence spectroscopy and contact angle measurements. We discuss the orientation of the molecules in terms of the tilt angle of the transition dipoles with respect to the surface. The topography of the films was characterized at the nanometre level by atomic force microscopy (AFM). The SHG behavior of the molecules was measured and the quality of the films was inferred from its angle dependence.

We found that the LB films of molecules (**2a**, **2b** and **2d**) are of Z-type and are highly NLO-active. Furthermore, one can deposit alternating Y-type LB layers of **2a** (or **2b**) and **2d**, which have the same NLO chromophore tethered at opposite extremities of the molecule. Thus one can avoid use of a non-active buffer layer required in the deposition of non-centrosymmetric Y-type LB films, using a NLO-active layer instead.

Experimental

Compounds **2a–2d** were synthesized according to the general procedure.[7] Their structures and purity was confirmed by ^{1}H and ^{13}C NMR spectra, HRMS and elemental analyses. Full synthetic details will be given elsewhere. Compounds **2a** and **2b** were purified by crystallization from acetic acid and compounds **2c** and **2d** chromatographically on a silica gel column using methylene chloride as eluent. Chloroform of analytical grade (Frutarom) was used as the spreading solvent (typically at a dye concentration of 0.5 mg ml^{-1}). Ultrapure water (resistivity 18 MΩ-cm) obtained from a Barnsted E-pure water purifier was used as the subphase. A modular dual trough from Labcon Ltd was used for surface pressure–area (π–A) measurements and LB film deposition. π–A isotherms of the Langmuir films were measured 30 min (or later) after spreading, to ensure evaporation of the solvent and equilibration of the film. Typically the compression and expansion were carried out at a rate of 5 mm^2 min^{-1}. Measurements were done at 11–32 °C and several pH values.

Deposition of the LB films was carried out at least 30 min after setting a desired surface pressure to allow relaxation of the film. Deposition was performed on to either a hydrophilic or hydrophobic glass slide at a speed of 5 mm min^{-1} for both up and down strokes. Sufficient time (~20 min) was allowed for drying the film between successive cycles. The glass slides were first cleaned with piranha solution (H_2SO_4–H_2O_2, 3 : 1) at 90 °C for 1 h, followed by repeated alternating water and acetone rinses, and finally dried in air for 12 h. Hydrophobic slides were produced by immersing the clean glass slides in octyltrichlorosilane (OTS) solution in dodecane for 1–2 h and then rinsing three times with ethanol.

Absorption spectra were recorded with a 8452A HP diode array spectrophotometer or a double beam JASCO, V-560 UV–Vis spectrophotometer. Polarized absorption spectroscopy was measured at varying incidence angles. Fluorescence emission spectra were recorded on a Jobin Yvon Fluorolog–2. The contact angles of the LB films were measured with a Goniometer (EVMA, model G-1, Erma INL, Japan). Ellipsometry was carried out on a variable angle spectroscopic ellipsometer VASE (Woollam Co., Inc, USA). Atomic force microscopy of the LB films was performed on a Dimension 3100 SPM (Digital Instruments Veeco) in tapping mode in air at room temperature.

Second harmonic generation of the LB films was measured with a 1064 nm, 35 ps laser (Surelite II, *Continuum Pico Yag*). A PMT with interference filters (532 nm transmission) was

used to collect the SHG signal. The LB films were rotated to approximately 45° relative to the incident laser beam. All measurements were referenced to an SHG signal obtained simultaneously from a thin BBO crystal plate.

Results and discussion

π–A isotherms

The π–A isotherms of compound **2a** on pure water (pH 5.5) in the temperature range 11–32 °C is shown in Fig. 3. The isotherms at the higher temperatures, 28 °C and 32 °C, show a low pressure, 2D liquid-expanded phase followed by a liquid-condensed or solid region, which collapses slightly below 50 mN m^{-1}. The limiting molecular areas obtained by extrapolation of the isotherms to zero surface pressure are 0.58 and 0.65 nm^2, respectively. At lower temperatures, the liquid expanded region practically disappears, with only the liquid-condensed or solid-like phases remaining evident before the collapse above 50 mN m^{-1}. The limiting molecular areas measured from these isotherms are 0.57 (22 °C), 0.6 (15 °C) and 0.59 (11 °C) nm^2 ($\pm$0.02 nm^2), respectively, and are similar to that measured for the prototype molecule **1** which we studied previously.[5,6] The Langmuir film of the dicarboxylic derivative is more rigid than that of the prototype molecule, as judged from the higher collapse pressure (30–50 mN m^{-1} compared to 25–35 mN m^{-1}), and the limited manifestation of the expanded phase.

The increase of the collapse pressure with decreasing temperature was also observed previously,[5,6] and can be understood in terms of a more ordered arrangement of the hydrocarbon chains at lower temperatures. Within the experimental uncertainty of our results, the molecular areas and surface pressures at which the liquid-expanded to liquid-condensed or solid transition takes place, were independent of temperature. The isotherms were independent of the time delay (up to 4 h) between spreading of the film and recording of the isotherms, indicating sufficiently rapid equilibration. The alternative possibility, of a relaxation slower than the time scale of the experiment, is ruled out on the basis of the reversibility of the isotherms below the collapse pressure.

The analogous molecule **2b** with one additional double bond in the π bridge, behaved roughly similarly to **2a**, except that the isotherm was "softer" (Fig. 4), retaining a liquid-expanded region even at the lower temperature. In agreement with this, also the collapse pressure was a little smaller than that observed for **2a**. The molecular areas are similar in both cases within the experimental uncertainty, as expected.

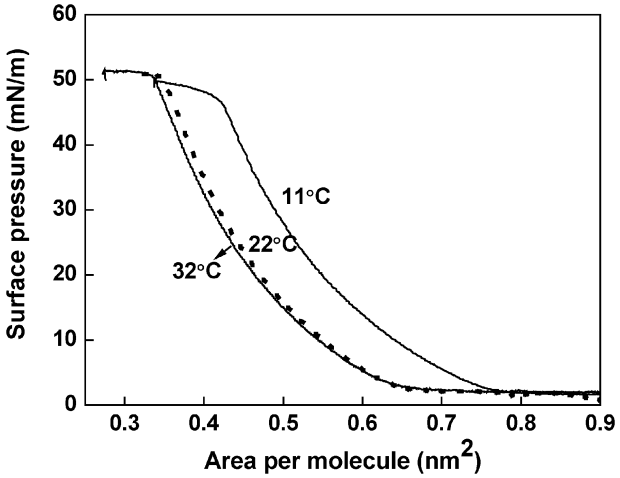

Fig. 4 Surface pressure–area isotherms of compound **2b** at different temperatures.

Below the collapse pressure the isotherms were essentially reversible, in line with the fast equilibration we mentioned above. However, when driving the films beyond their collapse, a hysteresis sets in both for **2a** and **2b** (figures not shown here), indicating irreversible loss of material.

The longer-term stability of the Langmuir monolayers was investigated by holding them compressed at a given surface pressure below collapse (say 25 mN m^{-1}). The films of derivative **2a** turned out to be very stable, showing no change in area even after 12 h of compression. The films of derivative **2b** were also found to be stable, manifesting after 12 h a surface area decrease of 2.1%, of the initial film area.

Fig. 5 shows that the surface behavior of **2a** at temperature of 11 °C is independent of the pH of the subphase below (pH 2.5) and above (pH 5.5) the pK_a values of the molecule (found by titration to be 2.6 and 4.4). However, when 2 × 10^{-4} M cadmium chloride was present in the subphase a transition to a somewhat lower molecular area structure was observed in the isotherm. This was especially apparent at a pH above the dissociation of the carboxylates, when one would expect a more pronounced interaction of the Cd ions with the charged carboxylates.

The smaller molecular area suggests an upright orientation of the molecules in the film, which is consistent with a more favorable alignment of the carboxylate groups with respect to the cadmium ions located in the subphase. In this alignment the main planes of the molecules (the conjugated π-ring

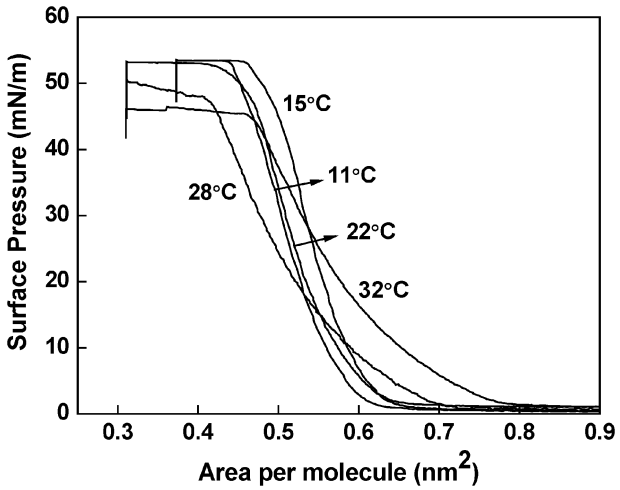

Fig. 3 Surface pressure–area isotherms of compound **2a** at different temperatures.

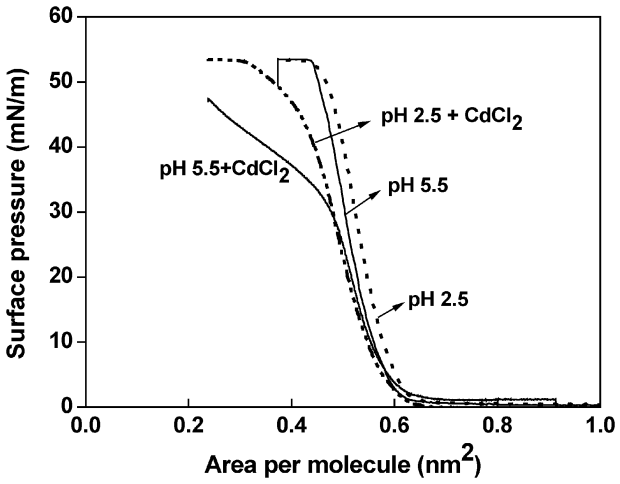

Fig. 5 Surface pressure–area isotherms of compound **2a** at different subphase pH values and in the presence and absence of 2 × 10^{-4} M $CdCl_2$, at 11 °C.

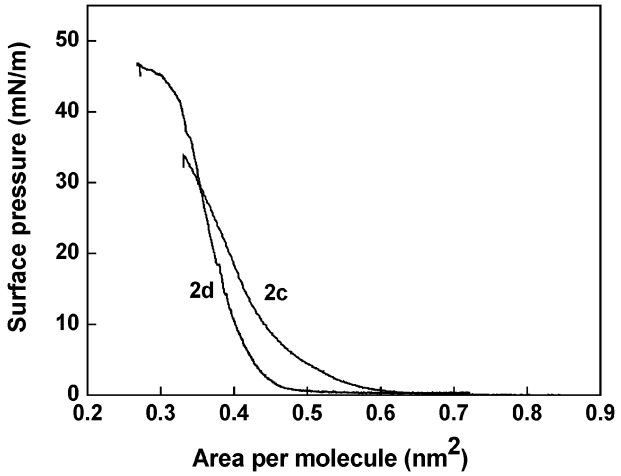

Fig. 6 Surface pressure–area isotherms of molecules **2c** and **2d** at 22 °C.

systems) are mutually parallel, as one would expect in their 3D crystals. Hence, the lower collapse pressure was measured in this case compared to the cases when cadmium salt was absent or at low pH (48 mN m^{-1} compared to 53 mN m^{-1}). We found that derivative **2b** easily undergoes protonation at the amino group and the conjugated bridge, whereas the long wave charge transfer band disappears. This compound is also reactive toward bases and its characteristic color disappears at pH higher than 6. Details on the acidic and basic properties of derivatives **1** and **2** in solution will be published elsewhere.

Fig. 6 shows the π–A isotherms of molecules **2c** and **2d** at 22 °C. The isotherm of **2c** goes through a liquid expanded to liquid condensed state and collapses at a pressure of 33 mN m^{-1}. The lower collapse pressure compared to that of **2d** may involve disordered Langmuir layers of **2c** perhaps owing to local crystallization at the air–water interface. Correspondingly, in the attempt to deposit LB films of **2c** we obtained a very low transfer ratio (0.3), even in the first down-stroke. We failed to deposit LB films of **2c** under a variety of deposition conditions and on to both hydrophilic and hydrophobic slides. Mixing **2c** with a long chain fatty acid, such as stearic acid (0.2 mole fraction), gave a stable isotherm with a larger collapse pressure. This kind of mixed monolayer gave essentially Y-type LB films, which were not suitable for SHG owing to their bulk centrosymmetric structure. It seems from the above results that strong interactions between **2c** molecules compared to the molecule–subphase interactions prevent LB deposition. With this in mind, **2d** was designed to involve a more hydrophilic head-group, replacing both methyl groups by the more hydrophilic acetoxyethylene groups. This was expected to provide stronger molecule–water interactions, and to overcome the problems set by **2c**.

In the π–A isotherm of **2d**, the liquid-expanded region practically disappeared with the only liquid-condensed or solid-like states being evident, followed by collapse at pressures above 45 mN m^{-1}. The steeper slope and increase of the collapse pressure attest to a more ordered 2D arrangement of the molecules in the film. The limiting area per molecule in this case was 0.41 nm^2, which was small compared to molecule **2c** (as well as **2a** and **2b**). LB films of **2d** can be deposited as Z-type LB films. The contact angle of the films was found to be 84°, *i.e.* they have a hydrophobic nature, in line with the Z-type deposition.

Langmuir–Blodgett films

Z-type LB films of **2a** (deposition took place only on the up-stroke) on hydrophilic glass slides were deposited at two extreme temperatures, 11 and 32 °C. The films were rather hydrophobic as revealed by the contact angle measurement (67°), with the chromophore head-groups pointing toward the glass substrate and the alkyl chains protruding outwards. We investigated various conditions for deposition of films of **2a** and **2b** (Table 1). Both compounds easily formed LB films with high transfer ratios (above 0.9), though **2a** was slightly better than **2b**. Understandably, surface pressures in the condensed phase are optimal for deposition, as long as one does not exceed the collapse pressure.

Table 1 LB film deposition conditions and transfer ratios

	Deposition conditions		
Compound	Temperature/°C	Surface pressure, π/mN m^{-1}	Transfer ratio[a]
2a	11	10	0.9–0.92↑
	11	25	0.98–1↑
	11	40	1–1.05↑
	32	25	0.9↑
2b	11	25	0.2↓–0.95–1↑
	32	25	0.4–0.5↓–0.9↑
2d	22	10	0.93–0.97↑
	22	30	0.93–1.0↑

[a] ↑ Up-stroke; ↓ down stroke.

The UV–Vis transmission–absorption spectra of **2a** in solution and in LB films of varying thickness lifted at 11 °C and 40 mN m^{-1} are shown in Fig. 7. The absorption spectra of the films indicate a uniform transfer of the molecules. Compared to a solution in chloroform, the absorption maxima of the LB films are significantly blue-shifted from 510 nm to 480 nm. The full widths at half maximum (FWHM) of the spectra of the LB films (for 10 layers, 100 nm) are considerably broader than the absorption band in solution (FWHM = 50 nm). The changes in the position and widths are indications of the relatively strong (non-uniform) interactions between the molecules within the compact films.

A careful examination of the spectra of the LB films showed that there are two main transitions (see deconvolution in Fig. 8). The weaker one appears near the position of the band in solution, and a stronger one blue-shifted to 480 nm. A third very weak feature was observed sometimes at higher energy, ~375 nm. The two main transitions are even more clearly manifested in the emission spectra (Fig. 9).

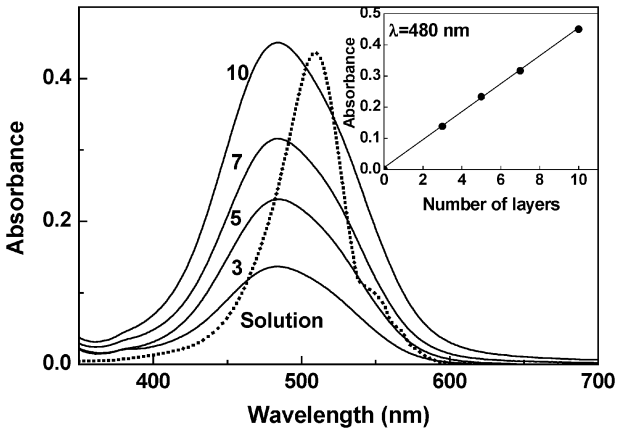

Fig. 7 UV–Vis absorption spectra of LB films of **2a** deposited at 11 °C and 40 mN m^{-1}. The numbers denote the number of layers on each side of the glass slide. The dotted spectrum is that of a 10^{-6} M solution of **2a** in $CHCl_3$. Inset—absorbance (at the maximum) *vs.* the number of layers in the film.

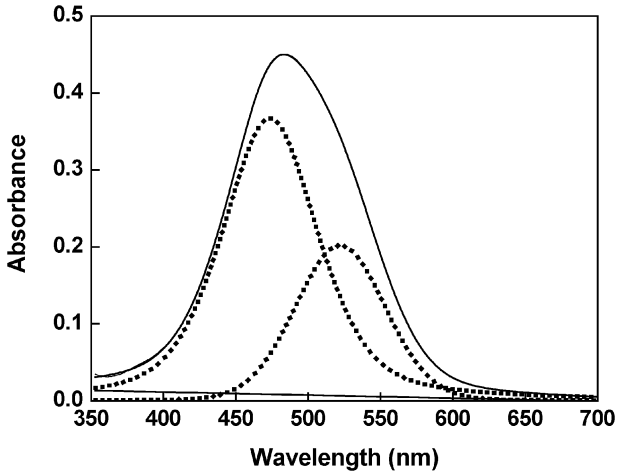

Fig. 8 Deconvolution of the UV–Vis absorption spectrum of 10-layer LB film of **2a** deposited at surface pressure 40 mN m^{-1} and 11 °C.

In compound **2a**, the major transition dipoles lie essentially along the major axis of the molecule. This is inferred from the donor–π–acceptor structure of the chromophore and was confirmed by quantum mechanical calculations, using the *N*,*N*-dimethylamino analog of **1** as a model in our previous paper.[5,6] Three singlet long wavelength transitions were calculated for an isolated molecule.

We carried out additional calculations on an analog of molecules **2**, (**3** in Fig. 10) using CIS (12 × 12) PM3, ZINDO and TD B3LYP/6-31G(d,p) model chemistries on the PM3 optimized geometry.[9] All three methods predicted that the low energy intense absorption band corresponds to a HOMO–$LUMO^{+1}$ transition: 376 nm (f = 0.8) (CIS PM3), 374 nm (f = 0.86) (ZINDO) and 433 nm (0.67) (TD B3LYP). The $LUMO^{+1}$ is localized mostly on the phthalic anhydride moiety of **3**. The HOMO–LUMO transition was predicted to be of low intensity by all methods, but whereas both of the semiempirical methods yielded a high energy transition: 311 nm (f = 0.01) (CIS PM3), 344 nm (f = 0.12), the TD B3LYP calculation gave 518 nm (f = 0.01). The LUMO is localized mostly on the 1,3-indanedione moiety of **3**.

The shift and broadening of the spectrum of the chromophores in the LB films can be explained by exciton splitting in aggregates as formulated by Kasha *et al.*[10,11] The blue-shift observed in the absorption band may be attributed to the H-type aggregate of **2a** molecules in the LB films, where the molecules are closely packed and have definite relative orientations dictated by the surface and their stacking.[12] Since we did

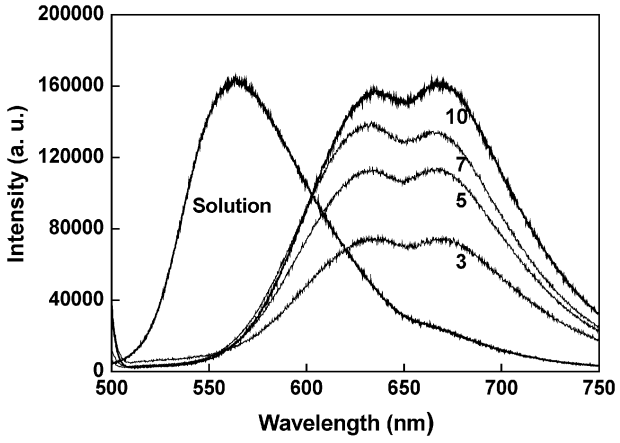

Fig. 9 Fluorescence spectra of **2a** in solution and in LB films of varying number of layers deposited at 40 mN m^{-1} and 11 °C, with excitation at 480 nm. The numbers denote the number of layers in the LB film.

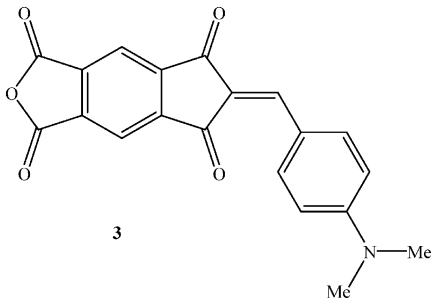

Fig. 10 Molecular structure of 6-[4-(dimethylamino)benzylidene]-1*H*-indeno[5,6-*c*]furan-1,3,5,7(6*H*)-tetrone (**3**).

not observe any significant change in the spectra of the LB films with an increasing number of layers, we inferred that the consecutive layers have nearly the same structure in terms of molecular conformation and packing.

In order to gain deeper insight into the spectroscopic behavior of the LB films, we performed CIS PM3 calculations also for oligomers of **3** (up to a hexamer). The oligomers were constructed by translating each molecule by 3.5 Å along the *z*-axis (perpendicular to the plane of the molecule) and by 2.9 Å along the *x*-axis (the long molecular axis) to approximate the tilt of the molecules in the LB film. The resulting molecular system for the hexamer is shown on Fig. 11.

In the CIS calculations, we included 4 × 4 orbitals for each molecule, which gives 4 × 4 for the monomer and 24 × 24 for the hexamer. We found that the energy of the HOMO–LUMO-type transitions does not practically depend on the number of molecules in the oligomer. However, the intense HOMO–$LUMO^{+1}$ transition of the monomer is always split into 2 transitions with f > 0.001 in the oligomers, not depending on the number of the interacting molecules. This is in line with the experimental results that showed two strong bands splitting out of the single band in solution. Of the two bands, the weaker transition becomes stronger upon increasing the number of the interacting molecules and after a bathochromic shift calculated for the dimer and trimer, returns back close to the position of the monomer for larger oligomers. The intense transition undergoes a steady hypsochromic shift, which reaches *ca.* 30 nm for the hexamer (Fig. 12).

The absorption spectra of molecule **2a** in LB films deposited at surface pressure 25 mN m^{-1} and temperature 32 °C along with the solution spectrum are presented in Fig. 13. At this temperature a smaller surface pressure was used for deposition since the collapse pressure is lower than at 11 °C. In general the spectra are similar to those obtained at 11 °C and 40 mN m^{-1}. The spectra are also blue-shifted, to 490 nm. The smaller blue-shift compared to that observed for films deposited 11 °C indicates a looser packing of the molecules at higher temperature, as evident from the "softer" Langmuir isotherms themselves.

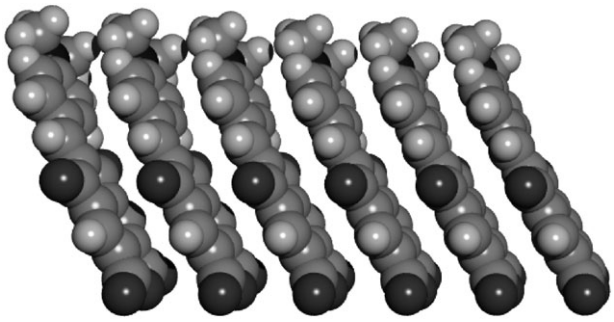

Fig. 11 Packing model of molecules **3** used in the calculations of the major electronic transitions.

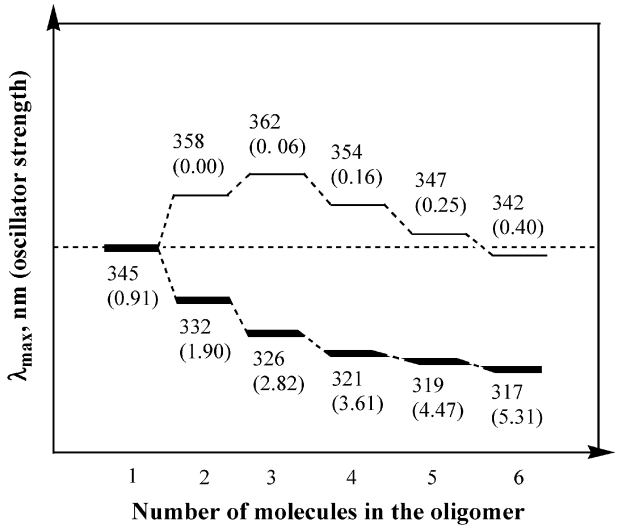

Fig. 12 Calculated wavelengths and intensities of the lowest energy electronic transitions in the oligomers of **3**.

The dependence of the optical density of the absorption band maximum on the number of layers at the two temperatures is shown in insets to Figs. 7 and 13. In both cases a linear dependence was observed indicating a uniform transfer of the layers. The optical density of the LB films deposited at 32 °C was much smaller (over five-fold) than for those deposited at 11 °C, which qualitatively corresponds to the less compact layers at the higher temperature. However, quantitatively the effect appeared to be too large to be explained by this effect alone.

The effect of the deposition pressure on 10 layers of LB films of **2a**, as manifested in their absorption spectra, showed an increasing absorption with increasing pressure (Fig. 14). The constant absorption maxima at 480 nm and the widths suggest that proximity interactions between the neighboring molecules hardly change, while the overall order and orientation improve at higher pressure.

Polarized absorption spectra were recorded at different incident angles (30°, 45°, and 60° between the direction of the incident light and the normal to the surface of the LB films). The spectra for s (perpendicular to the plane of incidence) and p (parallel to the plane of incident) polarization, I_s and I_p, are shown in Fig. 15. As expected the s-polarized spectrum was independent of the angle of incidence. Similarly, at normal incidence the p- and s- polarized spectra were identical within the experimental uncertainty.

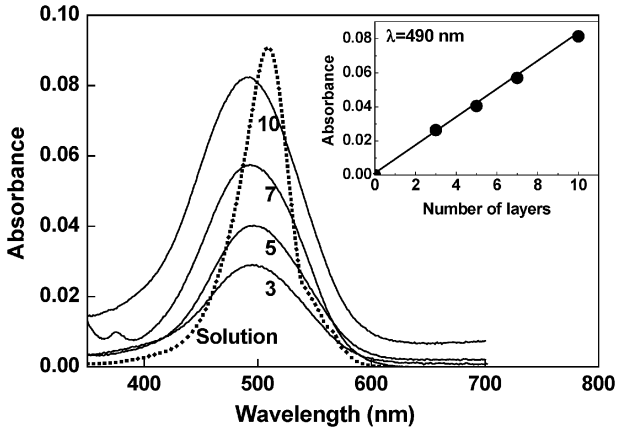

Fig. 13 UV–Vis absorption spectra of LB films of **2a** deposited at 32 °C and 25 mN m^{-1}. The numbers denote the number of layers on each side of the glass slide. The dotted spectrum is that of a 4.8×10^{-6} M solution of **2a** in $CHCl_3$. Inset—absorbance (at the maximum) *vs.* the number of layers in the film.

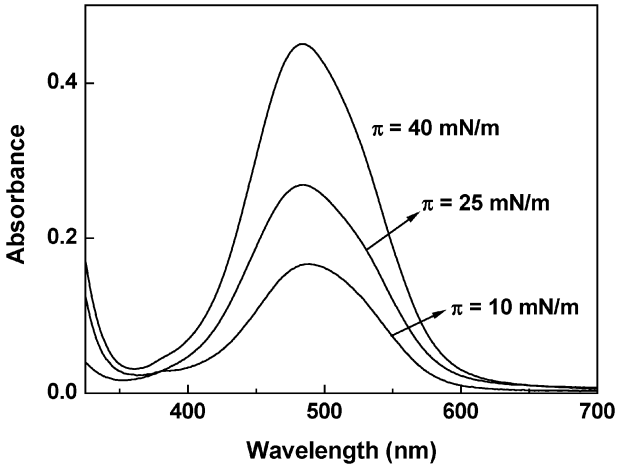

Fig. 14 UV–Vis absorption spectra of 10-layer LB films of compound **2a** deposited at 11 °C and at different surface pressures.

The analysis of the polarized spectra is based on the dichroic relation

$$(1 - 10^{-OD_p} f_p)/(1 - 10^{-OD_s} f_s)(1/\cos^2\alpha) = \tan^2\alpha + 2\cot^2\theta \quad (1)$$

OD_p and OD_s are the optical density of the p and s polarized spectra, respectively. θ is the tilt of the transition dipole with respect to the normal to the surface. α is the angle between the direction of incidence and the surface itself. We assume that all azimuthal angles (with a fixed angle, θ, between the transition dipole and normal to the surface) are equally probable. f_p and f_s correct the 10^{-OD} terms for the dependence of the reflectivity from the film coated glass slide on the angle of incidence for the low polarizations (see ESI).†

The dependence of $\{(1-10^{-Ip} f_p)/(1-10^{-Is} f_s)\}(1/\cos^2\alpha)$ on $\tan^2\alpha$ for the 480 nm band for molecule **2a** deposited at three different surface pressures at 11 °C is shown in Fig. 16. The average orientation of the chromophore with respect to the surface normal, θ, is calculated from the intercept, 55 ± 1°.

Fig. 9 shows the fluorescence emission spectra of **2a** in chloroform and in LB films deposited at 11 °C and 40 mN m^{-1}. The solution emission spectrum shows an intense band at about 565 nm. In the LB films the spectra are considerably red-shifted and exhibit two bands, centered at 633 nm and 668 nm. The Stokes shift is a manifestation of the fundamental difference between the molecular environment in the films compared to solution—*i.e.* the absence of the solvent and the close proximity of the chromophores to each other. The results were in agreement with the results obtained for vacuum deposited

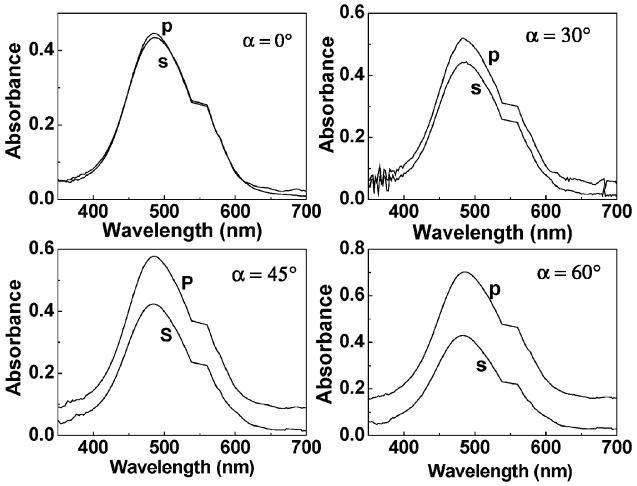

Fig. 15 Polarized absorption spectra of 10-layer LB film of compound **2a** deposited at 40 mN m^{-1} and 11 °C at different angles of incidence.

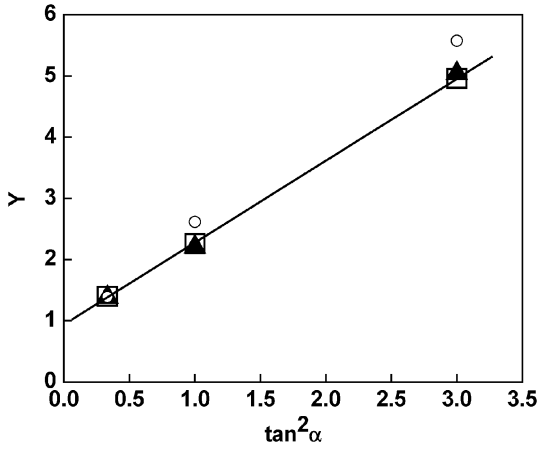

Fig. 16 Analysis of polarized absorption spectra of the LB films of **2a** deposited at different surface pressures: 40 mN m^{-1} (open squares), 25 mN m^{-1} (solid triangles) and 10 mN m^{-1} (open circles) including the transmittance correction. $Y = [\{1 - 10^{-OD_p} f_p(\alpha'')\}/\{1 - 10^{-OD_s} f_s(\alpha'')\}] \times (1/\cos^2\alpha)$; α is the angle between the direction of incidence of light and the LB film surface.

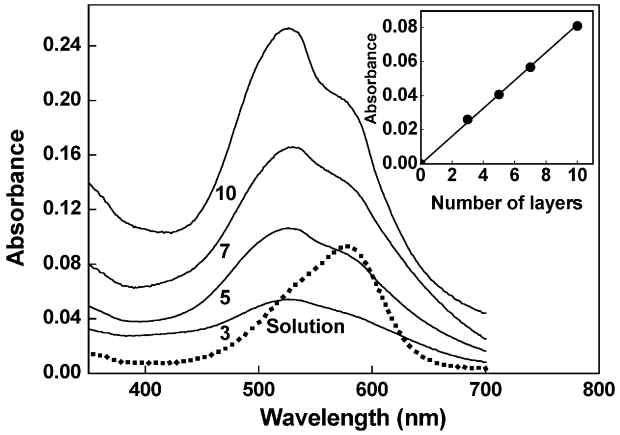

Fig. 18 UV–Vis absorption spectra of **2b** in solution and in LB films deposited at 25 mN m^{-1} and 25 °C. The number of layers is given near each curve. Inset—the maximum of absorbance as a function of the number of layers.

films of related compounds, DMABI.[13,14] The fluorescence spectra do not change in shape with increase of the number of layers, indicating that intermolecular interactions within the layers are dominant compared to interactions between layers, in line with the π-stacking discussed above.

The fluorescence spectra of the LB films of **2a** at different surface pressures are given in Fig. 17. The spectra are essentially the same for all pressures in the range 10–40 mN m^{-1}. This agrees with the corresponding absorption spectra that did not show any significant variation either. The long fluorescence tail in the blue side of the spectrum for 10 mN m^{-1} deposition plausibly means that these films are not as ordered as those formed at the higher pressures.

The spectra of the LB films of compound **2b** deposited on a hydrophilic slide at 25 mN m^{-1} and 11 °C are shown in Fig. 18. Compared to **2a** the individual two bands are more prominent, and the change in their relative intensities is also more pronounced. The linear dichroism of the **2b**-LB films gave an average tilt angle of 50 ± 1°.

Derivative **2b** deposited mostly in the up-stroke, similarly to **2a**, but unlike the latter it also manifested some deposition in the down-stroke (0.2 at 11 °C and 0.4–0.5 at 32 °C). This point is of interest as derivative **2b** differs from derivative **2a** by merely one double bond in the bridge between the same donor and acceptor moieties. In spite of the apparent (partial) two-way deposition, the films of **2b** were invariably hydrophobic (as evidenced by the contact angle of 72°). Thus it seems that also in this case the Z-type films formed, perhaps *via* rearrangements of the molecules within the film. This is apparent also from the finite SHG signals measured from these films (see below).

Derivative **2b** showed a similar fluorescence spectrum to that of derivative **2a** (not shown) in spite of the difference in their absorption spectra. While the absorption bands of **2b** are red-shifted with respect to those of **2a** their fluorescence spectra nearly overlap.

Tapping-mode AFM images of 3-layer LB films of **2a** and **2b** deposited at 11 °C and at a surface pressure of 40 mN m^{-1} and 25 mN m^{-1}, respectively are shown in Figs. 19 and 20. Both molecules seem to deposit in islands with **2a** apparently forming larger regions compared to **2b**. The depth profile of the images exhibited height variations of 10–12 nm, indicating an average monolayer thickness of **2a** of ~4 ± 1 nm. This is slightly larger than the expected layer width of ~3 nm (estimated on the basis of 2.1 nm alkyl chain length, the 1.6 nm extent of the chromophore, and a tilt of 50°). Ellipsometry of 5 layers gave as best fit a total thickness of 30.1 ± 1.1 nm (and the refractive index of 1.343 ± 0.016), *i.e.* 6.0 ± 0.2 nm per layer, somewhat larger than the AFM result. This difference is

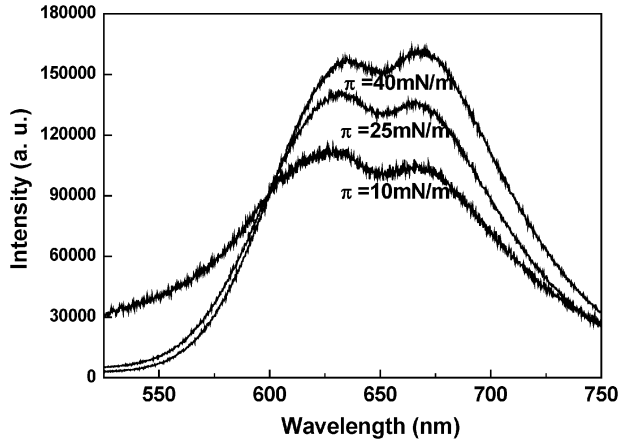

Fig. 17 Emission spectra of a 10-layer LB film of **2a** deposited at different surface pressure at 11 °C.

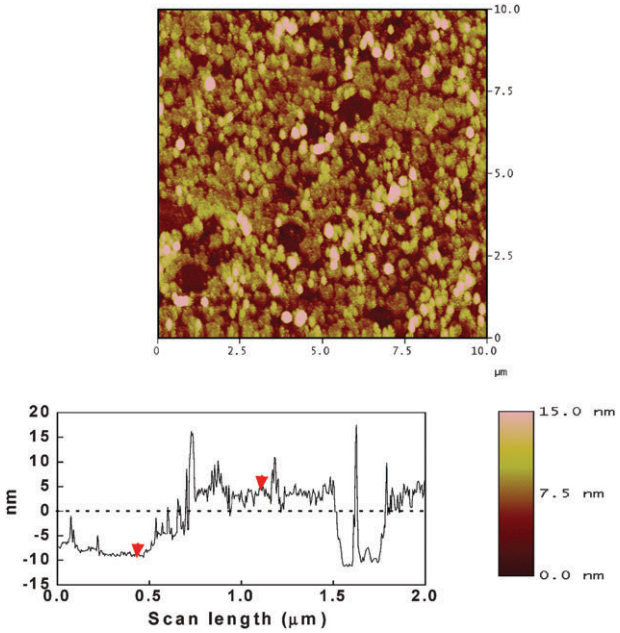

Fig. 19 AFM topography and height profile of compound **2a** in a 3-layer LB film deposited at 40 mN m^{-1} and 11 °C.

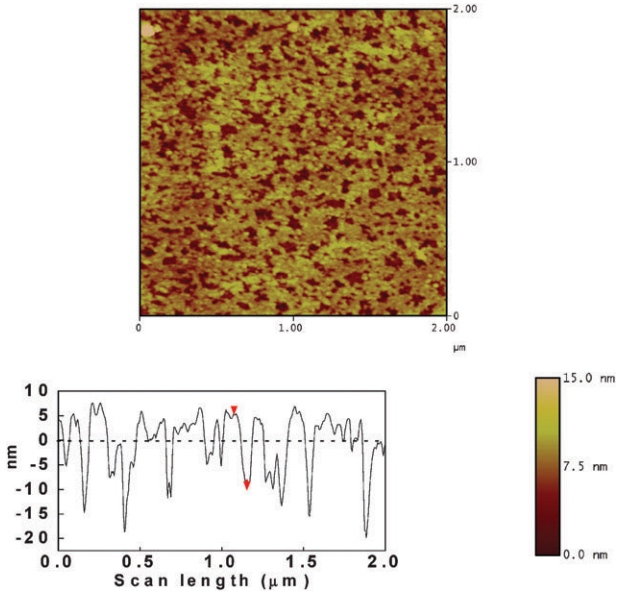

Fig. 20 AFM topography and height profile of compound **2b** in a 3-layer LB film deposited at 25 mN m^{-1} and 11 °C.

reasonable considering the model dependence of the analysis of the ellipsometry results. The thickness of each monolayer of **2b** in the LB film was found from the depth profile of the AFM measurements to be 5–6 nm. This, again, is reasonable considering the molecular dimensions.

Molecule **2d** behaved similarly to **2a** and **2b** in terms of its deposition in LB films, its surface absorption and fluorescence.

Second harmonic generation measurements

The 532 nm SHG signal obtained from 1064 nm radiation incident on the **2a** and **2b** LB films was measured from the fringes resulting from the interference of the SHG signals generated by the film on the two sides of the glass substrate. p-Polarization was used for both incident and SHG beams. A typical fringe for a 5-layer LB film of **2a** deposited at 40 mN m^{-1} and 11 °C is shown in Fig. 21.

The SHG signals (normalized to the maximal SHG signal from a 1 mm quartz plate (χ_{11}) at ~45° incidence angle) of 10-layer LB films of molecule **2a** deposited at various surface pressures at 11 °C and 32 °C are summarized in Table 2. The strongest intensity was observed for the LB film deposited at the surface pressure of 40 mN m^{-1} at 11 °C, indicating relatively high order. The LB film deposited at 32 °C and 25 mN m^{-1} had a very low efficiency and fluorescence, which we did not observe from the other films.

Table 2 SHG from 10-layer LB films of **2a** prepared at different deposition conditions

Surface pressure/mN m^{-1}	Temperature/°C	SHG signal[a]
40	11	2.66×10^{-2}
25	11	2.16×10^{-2}
10	11	1.93×10^{-2}
25	32	4.01×10^{-3}

[a] Maximum fringe SHG signal normalized to a SHG signal from a thin quartz crystal. Experimental uncertainty is ±0.0007.

Table 3 SHG from different number of layers of **2a** deposited at 40 mN m^{-1} and 11 °C[a]

Number of layers	Fresh	Two weeks old films
3	1.62×10^{-2}	5.9×10^{-4}
5	2.33×10^{-2}	7.69×10^{-4}
7	1.40×10^{-2}	3.70×10^{-4}
10	2.66×10^{-2}	1.37×10^{-3}

[a] Experimental uncertainty is ± 0.0007.

The SHG signal seemed to increase with the number of layers (Table 3). In ideal and uniform layers the SH signal should increase quadratically with their number. However, the dependence was weak, and large deviations from the expected trend were observed. The 7-layer film was noticeably out of line and was probably highly defective. We attribute this imperfect behavior to disorder in the films, as is evidenced also from the fact that the SHG fringes did not decrease to zero (Fig. 22).

The films deteriorated strongly with time, in a matter of days, as evidenced by the decline of the SHG signals (Table 3) and the absorption spectra (not shown). The analogous molecule **2b** behaved similarly to **2a** with overall lower signals. Indeed, as remarked above, these films were less ordered than those of molecule **2a**. The signal from a 3-layer Z-type LB film of **2a** is comparable to the signal we measured from an 8-layer alternating Y-type film of this molecule,[5] both being as intense as the signal from quartz. Molecule **2d** also gave strong SHG signals, between those of **2a** and **2b**.

In order to avoid using an inert spacer layer required for deposition of Y-type non-centrosymmetric LB films, we used molecule **2d** together with **2a** (or **2b**) for deposition of the alternating LB films.[15–20] **2a** and **2d** have the same NLO chromophore tethered at opposite extremities of the molecule.

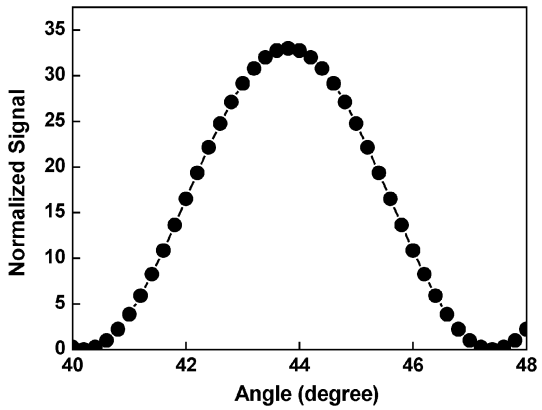

Fig. 21 Typical dependence of the second harmonic intensity on the angle of incidence of the laser beam. A 5-layer LB film of **2a** deposited at 11 °C and 40 mN m^{-1}.

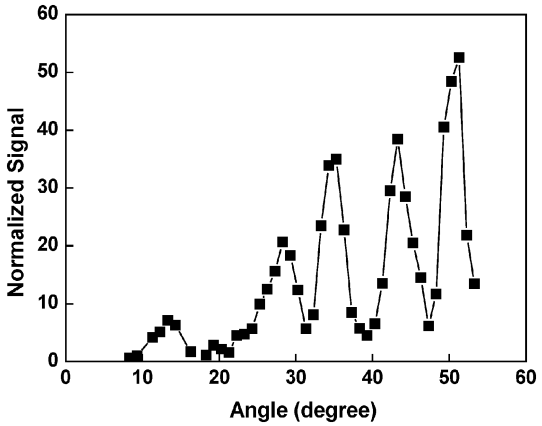

Fig. 22 SHG fringe for the second harmonic intensity as a function of angle of incidence for alternate LB films (5-layer each) of **2d** and **2a** deposited at 40 mN m^{-1} and 22 °C.

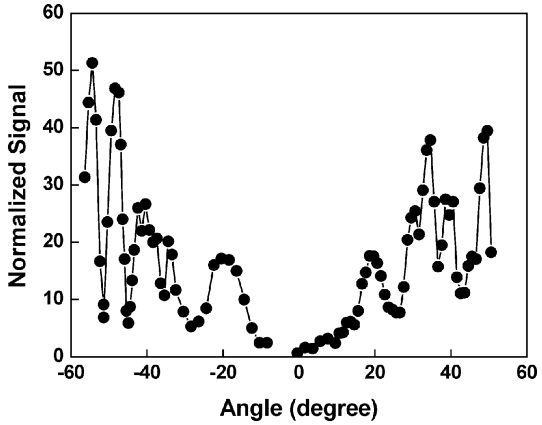

Fig. 23 SHG fringe for second harmonic intensity as a function of angle of incidence for alternate LB films (5-layer each) of **2d** and **2b** deposited at $\pi = 25$ mN m^{-1} and $T = 22$ °C.

Alternating films were produced by lifting the substrate through a Langmuir layer of **2d** and then lowering the substrate through a monolayer of either **2a** or **2b**. In this context one should note that Penner's group[15] reported the construction of related systems, involving LB films of two oppositely oriented NLO active LB chromophores anchored to polymers. They obtained stable ordered films with well-defined SHG behavior (as evidenced by interference SHG fringes). In our present work, the chromophores are individual molecules, with much larger intrinsic NLO coefficients. The typical fringe pattern of these films is shown in Figs. 22 and 23. The fringe pattern was pronounced and the signals were retained even after a couple of weeks, indicating stability of the films. However, the imperfect contrast between the maxima and minima in these fringes indicates defects in the films (or, less probably, differences in the films on both sides of the glass substrate). Recall that the LB films of **2a**, **2b** or **2d** by themselves are of Z-type, which are, in general, less stable than the Y-type due to the unstable hydrophilic–hydrophobic interaction between the adjacent monolayers. Thus, the alternating Y-type films with the non-centrosymmetric layout described here might be more useful for engineering of the NLO thin films.

Conclusions

In this report we discussed the surface behavior of several NLO-active amphiphilic chromophores based on the A–π–D structure, and the LB films formed from them. The final goal was to obtain the NLO-active LB films within which the chromophores have definite orientation. Polarized absorption spectra, AFM and ellipsometry measurements showed that the molecular transition dipoles in the film have a (molecule dependent) tilt angle of 40° to 50° with respect to the surface normal. The structure of the LB films was only slightly affected by inclusion of the additional double bond into the bridge between the two conjugated D and A moieties. Spectroscopic and microscopic studies suggested formation of aggregates in the LB films. We produced Z-type single component films and Y-type two component alternating films. Strong SHG signals stable over weeks, especially in the alternate-layer LB films, were observed.

Acknowledgements

We thank the Harry Stern fund for partial financial support. The authors are thankful to Dr L. Shapiro for the technical help and useful discussions.

References

1 L. Gaffo, C. J. L. Constantino, W. C. Moreira, R. F. Aroka and O. N. Oliveira Jr, *Langmuir*, 2002, **18**, 3561.
2 L. J. Kloeppner and R. S. Duran, *J. Am. Chem. Soc.*, 1999, **121**, 8108.
3 (*a*) *Molecular Nonlinear optics: Materials, Physics and Devices*, ed. J. Zyss, Academic Press, Boston, 1994; (*b*) K. B. Eisenthal, *Chem. Rev.*, 1996, **96**, 1343.
4 H. S. Nalwa and M. Seizo, *Nonlinear Optics of Organic Molecules and Polymers*, CRC Press, Boca Raton, FL, 1994.
5 H. Schwartz, R. Mazor, V. Khodorkovsky, L. Shapiro, J. T. Klug, E. Kovalev, G. Meshulam, G. Berkovic, Z. Kotler and S. Efrima, *J. Phys. Chem. B*, 2001, **105**, 5914.
6 H. Schwartz, P. Krief, J. Y. Becker, L. Shapiro, V. Khodorkovsky, J. T. Klug, E. Kovalev, G. Meshulam, G. Berkovic, Z. Kotler and S. Efrima, *Proc. SPIE*, 2002, **4798**, 105.
7 P. Krief, J. Y. Becker, A. Ellern, V. Khodorkovsky, O. Neilands (late) and L. Shapiro, *Synthesis*, 2004, **15**, 2509.
8 M. R. Christopher, T. J. Twieg, V. Y. Lee, S. A. Swanson, B. M. Kathleen and M. D. Robert, *J. Am. Chem. Soc.*, 1993, **115**(26), 12599.
9 M. J. Frisch, G. W. Trucks, H. B. Schlegel, G. E. Scuseria, M. A. Robb, J. R. Cheeseman, V. G. Zakrzewski, J. A. Montgomery, R. E. Stratmann Jr., J. C. Burant, S. Dapprich, J. M. Millam, A. Daniels, K. N. Kudin, M. C. Strain, O. Farkas, J. Tomasi, V. Barone, M. Cossi, R. Cammi, B. Mennucci, C. Pomelli, C. Adamo, S. Clifford, J. Ochterski, G. A. Petersson, P. Y. Ayala, Q. Cui, K. Morokuma, D. K. Malick, A. D. Rabuck, K. Raghavachari, J. B. Foresman, J. Cioslowski, J. V. Ortiz, A. G. Baboul, B. B. Stefanov, G. Liu, A. Liashenko, P. Piskorz, I. Komaromi, R. Gomperts, R. L. Martin, D. J. Fox, T. Keith, M. A. Al-Laham, C. Y. Peng, A. Nanayakkara, M. Challacombe, P. M. W. Gill, B. Johnson, W. Chen, M. W. Wong, J. L. Andres, C. Gonzalez, M. Head-Gordon, E. S. Replogle and J. A. Pople, *GAUSSIAN 98, (Revision A.9)*, Gaussian Inc., Pittsburgh, PA, 1998.
10 M. Kasha, H. R. Rawls and M. A. El-Bayoumi, *Pure Appl. Chem.*, 1965, **11**, 371.
11 E. G. McRae and M. Kasha, *J. Chem. Phys.*, 1958, **28**, 721.
12 M. A. Rutkis, E. Wistus and S. E. Lindquist, *Proc. SPIE – Int. Soc. Opt. Eng.*, 1997, **2968**, 34.
13 V. Gulbinas, G. Kodis and L. Valkunas, *J. Phys. Chem.*, 1996, **100**, 19441.
14 S. Jersenas, A. Gruodis, G. Kodis, M. Chachisvilis, V. Gulbinas, E. A. Silinsh and L. Valkunas, *J. Phys. Chem.*, 1998, **102**, 1086.
15 H. R. Motschmann, T. L. Penner, N. J. Armstrong and M. C. Ezenyilimba, *J. Phys. Chem.*, 1993, **97**, 3933.
16 D. B. Neal, M. C. Petty, G. G. Roberts, M. M. Ahmad, W. J. Feast, I. R. Girliing, N. A. Cade, P. V. Kolonsky and I. R. Pewterson, *Electron Lett.*, 1986, **22**, 460.
17 R. C. Hall, G. A. Lindsay, B. Anderson, S. T. Kowel, B. G. Higgins and P. Stroeve, *Mater. Res. Soc. Symp. Proc.*, 1988, **109**, 351 (Nonlinear Opt. Prop. Polym.).
18 B. Anderson, R. C. Hall, B. G. Higgins, G. A. Lindsay, P. Stroeve and S. T. Kowel, *Synth. Mater.*, 1989, **28**, D711.
19 S. Desrousseaux, B. Bennetau, J. Morand, C. Mingotaud, J. F. Leterd, S. Montant and E. Freysz, *New J. Chem.*, 2000, **24**, 977.
20 K. Han, Q. Wang, G. Tang, H. Li, X. Sheng and Z. Huang, *Thin Solid Films*, 2005, **476**, 152.